Progress In Electromagnetics Research B, Vol. 39, 179–195, 2012

COMBLINE LOADINGS OF PRINTED TRIANGULAR MONOPOLE ANTENNAS FOR THE REALIZATION OF MULTI-BAND AND WIDEBAND CHARACTERISTICS

H. Oraizi and B. Rezaei*

Department of Electrical Engineering, Iran University of Science and Technology, Tehran, Iran

Abstract—In this paper, we use the concept of stub loadings of planar microstrip antennas to convert a single band antenna into a dual-band antenna used for WLAN. We load a planar triangular monopole (PTM) antenna by combline stubs attached to the edges of patch in order to obtain a second resonance frequency. The simple PTM antenna is first designed to produce the lower resonance frequency and the geometry of combline stubs is then optimally designed to generate the higher resonance frequency to realize a dual-band or a wideband antenna. Three prototype models of PTM antennas are designed, fabricated and measured. Their performances verify the concept of inductive loadings of planar antennas by combline stubs for the realization of dual-band and wideband performance for WLAN.

1. INTRODUCTION

The simple monopole antenna having low profile and omnidirectional radiation pattern is extensively used in communication systems. However, its main drawback is its narrow bandwidth. Extensive effort has been made to modify its structure for increasing its bandwidth. For example, the monopole wire antenna is changed into a printed version [1–4], such as the circular disk monopole antenna having $10:1$ bandwidth used in UWB systems [5]. The triangular monopole printed antenna is introduced in [6] and is shown to have a variable bandwidth as a function of its tapering angle. It may achieve a bandwidth of about 30% [7]. Furthermore, its bandwidth may be increased by some modifications in its ground plane, such as cutting various slot shapes in it. Bandwidths of 50% [8] and 77% [9] have been reported.

Received 11 January 2012, Accepted 5 March 2012, Scheduled 12 March 2012

* Corresponding author: Bahram Rezaei (b.rezaei.iust@gmail.com).

On the other hand, the antennas designed for applications in communication systems, such as WLAN and GSM should have acceptable performance in the specified frequency bands, rather than merely exhibit wide bandwidths outside the designed operation frequencies. Accordingly, in this paper we intend to design a dual band printed monopole antenna. The objective is to add an adjustable operation frequency band to the proposed antenna. Examples of antenna structures with multiband characteristics are PIFA [10] and stacked antenna [11], which suffer from being 3-dimensional (which leads to occupying a large space contrary to the prevalent trend for miniaturization) and complexity of fabrication (which is against the economic requirements of mass production of devices, such as mobile sets). The proposed structure consists of the inductive loading of triangular patch, which is fabricated by simple photolithography technology.

In this paper, we present a novel and simple planar structure for dual-band and wideband applications in WLAN systems. Narrow combline stubs are placed on the edges of patch to produce parallel inductive effects, which are due to the appearance of current distributions in the frequency bands other than in its basic design band. This configuration may lead to acceptable radiation behavior in two or more frequency bands. Since the proposed antenna is implemented in a planar microstrip structure, it is more robust and sturdy, may be easily fabricated and occupies less space than the other comparable antennas.

Having provided some brief introductory comments in Section 1, the proposed inductive loadings of the microstrip patch antenna is described in Section 2. The single-band planar triangular monopole (PTM) antenna is then designed for the first operation band of WLAN in Section 3. Subsequently, the method of designing PTM antennas for dual-band performance by stub loadings is explained in Section 4. The procedure for drawing the resonance frequencies closer together to produce wideband operation is described in Section 5. The fabricated prototype models of each case are explained and their performances (as obtained by full-wave simulation results and measurement data) are compared. Finally the concluding remarks are presented.

2. ANALYSIS AND DESIGN OF THE PTM ANTENNA

We intend to load a PTM antenna by combline stubs to obtain a dual-band antenna for WLAN system applications. The stub loading has no effect on the lower band, but produces a higher resonance band, as will be discussed in Section 3. Accordingly, we design a PTM antenna

for operation at 2.4 GHz as shown in Figure 1 and the second WLAN band is generated by stub loading [12–19]. The selected substrate is RT5880 (with $\varepsilon_r = 2.2$, height $= 0.787$ mm and $\tan\delta = 0.0009$). The ground plane is rectangular with limited dimensions ($L \times L_1$), for simulation and physical realization. The antenna feed is through a microstrip line of length L_2 and width W_1 (see Figure 1). It is connected to the triangular patch through a transition of length (L_2–L_1), which improves the impedance matching. The ground plane is rectangular and located under the feed line ($L \times L_1$), but does not extend up to the apex of patch. There is a short distance between the edge of ground plane and the apex of triangular patch. Therefore, the radiation patterns will be bidirectional, which is appropriate for WLAN

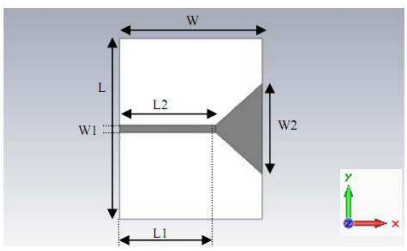

(a)

W	W_1	W_2	L	L_1	L_2
49	2.37	31.5	63	33.4	32.5

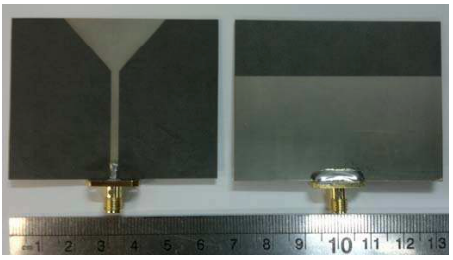

(b)

Figure 1. The PTM antenna. (a) Layout; (b) fabricated prototype. Dimensions are in millimeters.

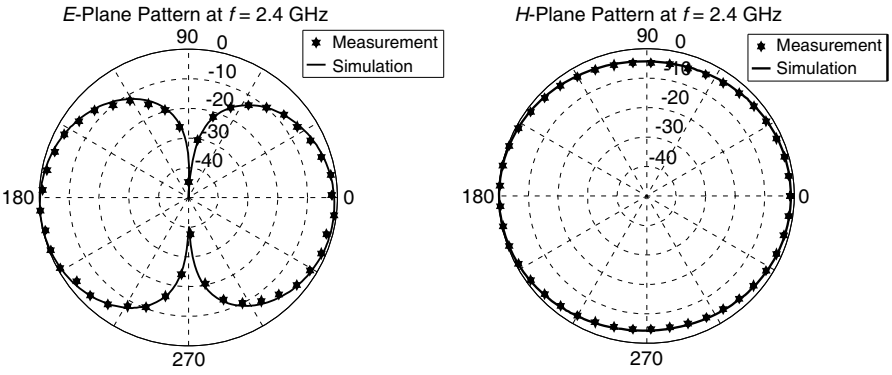

(a) (b)

Figure 2. The PTM antenna normalized pattern at 2.4 GHz. (a) E-plane (xoz); (b) H-plane (yoz).

applications. The CST full-wave software is used for the computer simulations.

The radiation patterns and reflection coefficient of PTM antenna are shown in Figures 2 and 3, respectively. Its frequency bandwidth is about 38% in the band 2.04 $\sim$ 3.01 GHz, for which the reflection coefficient is specified to be less than -10 dB. The antenna co polar gain is 3.1 dBi at 2.4 GHz. Since the finite ground plane and feed line are about a quarter wavelength long at 2.4 GHz, floating currents may be generated in the shield of coax cable connected to the under test antenna. Consequently, an isolator is used in the antenna input during the measurements.

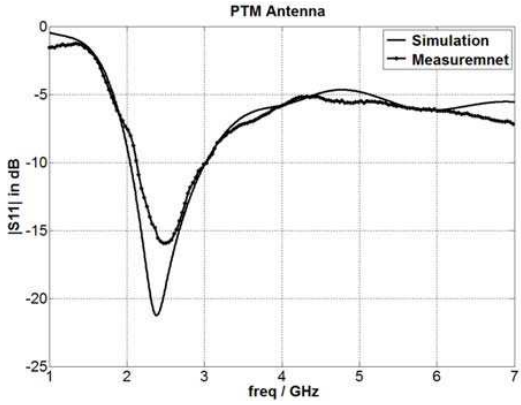

Figure 3. Simulated and measured reflection coefficients of the PTM antenna.

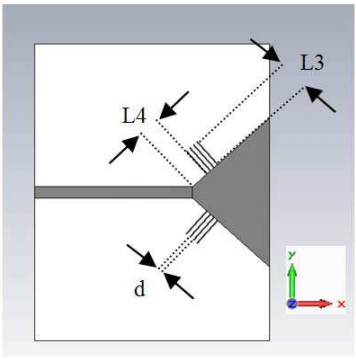

W	W_1	W_2	L	L_1	L_2	L_3	L_4	n
49	2.37	31.5	63	33.4	32.5	3.5	4	4

Figure 4. Loaded PTM antenna. Dimensions are in millimeters.

3. COMBLINE LOADINGS ON PTM ANTENNA

Open- and short circuited stubs may be used for the generation of inductive loadings. However, such a device requires a ground plane under the patch. The ground plane here doesn't extend under the proposed triangular antenna. Consequently we may not use such inductive loadings. We intend to design a dual band PTM antenna for WLAN applications. Therefore, we inductively load the PTM antenna by comblines on the tapered edges of triangular patch, to save some space as shown in Figure 4. The first resonance frequency is obtained by the design of the basic triangular patch. The second resonance frequency is obtained by appropriate evaluation of design parameters, such as lengths, widths, spacings, locations and number of stubs. The antenna may be designed by a parametric study through computer simulation.

We conducted a parametric study for the reflection coefficient of the triangular patch antenna with combline loadings in the frequency band $1 \sim 7$ GHz. The parameter sweep is made for the stub lengths (L_3), stub spacing (d), number of stubs (n) and off-set of stubs from the

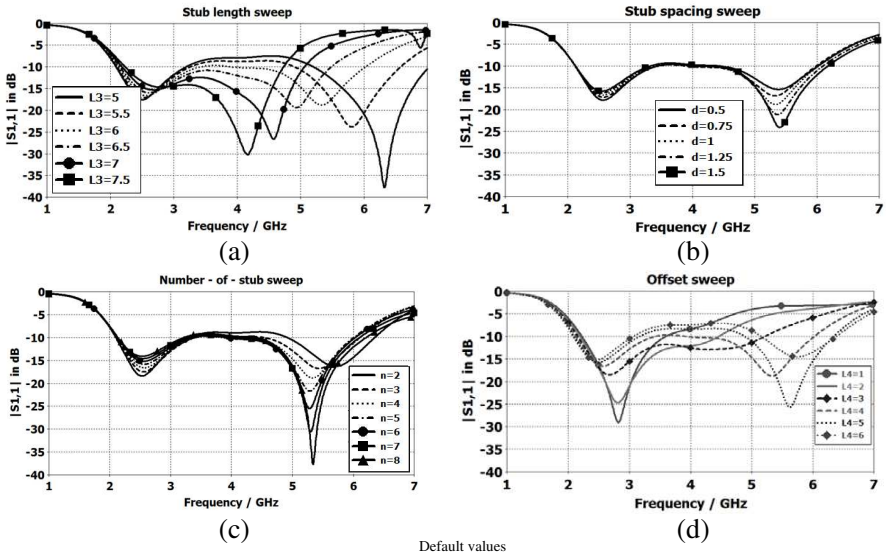

Default values

W	W_1	W_2	L	L_1	L_2	L_3	L_4	n
49	2.37	31.5	63	33.4	32.5	3.5	4	4

Figure 5. Parametric study for loaded PTM antenna. (a) stub length; (b) stub spacing; (c) number-of-stub; (d) stub offset. Dimensions are in millimeters.

apex (L_4). Their reflection coefficients (S_{11}) are shown in Figures 5(a)–(d), respectively.

We may obtain the following conclusions from the behavior of these figures:

1- Figure 5(a) indicates that the lower resonance frequency is approximately independent of stub lengths, but the higher frequency is inversely proportional to it. As the stub lengths increase, the two resonance frequencies approach and combine. Consequently, the lengths of stubs may be varied to adjust the second resonance frequency or obtain wideband characteristics from the antenna.

2- Figure 5(b) shows that the stub spacing does not have any significant effect on the locations of first and second resonance frequencies. However, it has some effect on the antenna impedance matching at both resonance frequencies, particularly at the upper one. The stub spacing may then be used as a fine tuning parameter for the antenna, whereas the stub length could be a coarse tuning factor.

3- Figure 5(c) indicates that the number of stubs has the same general effect as the stub spacing. Increasing the number of stubs improves the impedance matching at the higher resonance frequency. The reverse effect occurs at the lower resonance frequency.

4- Figure 5(d) displays that the offset location of stubs (L_4), similar to the stub lengths, has a significant effect on the second resonance frequency. The variation of this parameter may make the antenna exhibit dual-band or wideband characteristics. Namely, increasing the value of L_4 will make the antenna transit from dual-band to wideband performance.

Consequently, the two basic parameters, namely stub lengths and offset locations, may be used for the design of resonance frequencies and the other two parameters (namely, the number of stubs and their spacings) may be used for the improvement of impedance matching. To gain an understanding of the operation of the proposed antenna with stub loadings, we draw the current distributions of the basic PTM antenna and those of the stub loaded structure in Figure 6, at frequencies 2.4 GHz and 5 GHz, respectively.

Observe that at the lower operation frequency band, the current distributions on the stubs are negligible relative to that on the main body of the antenna. Therefore, the two antenna configurations (namely with and without stubs) are approximately similar with respect to current distribution and return loss. The current

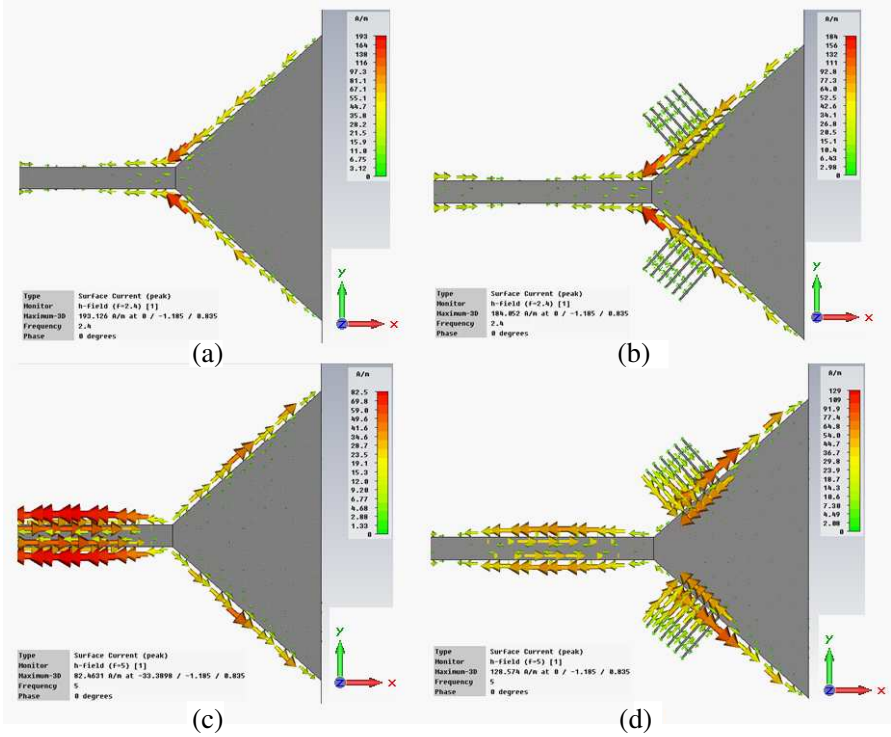

Figure 6. PTM antenna current distributions. At 2.4 GHz: (a) original; (b) stub loaded. At 5 GHz: (c) original; (d) stub loaded.

distributions on the stubs are directed in opposite directions, which may lead to the cancelation of their radiation effects along the normal direction. In the upper frequency portion of the band, as shown in Figures 6(c), (d), the intensity of current distributions is quite considerable on the stubs. They enhance each other's effects, because they are also codirectional. This is a favorable characteristics, because shorter stubs may be used resulting in some antenna miniaturization. Furthermore, such a current distribution on the stubs produces relatively strong magnetic fields and energy around the stubs, leading to effective inductive loadings of antenna.

On the other hand, the capacitive effects of the stubs are negligible, due to the absence of a ground plane under them and their thin thickness and wide spacings. Referring to Figure 5(d) and antenna dimensions, the overlap of combline stubs with the ground plane is appreciable for the case of L_4 equal to about 1 mm. however, in our antenna, only a part of the tip of first stub (less than 0.1 mm)

overlaps the ground plane. This may produce a capacitive effect, which is ignorable compared to the inductive loading.

The inductive loadings by stubs may be verified further by computer simulation. The open- and short-circuit termination of transmission lines may be modeled by capacitive and inductive elements. This model is used for the computer simulation of stubs, in order to show their inductive behavior.

In the computer models, the stubs are replaced by equivalent lumped elements and their terminals are connected to the remote plane ground by thin strips as shown in Figure 7.

It is observed that a capacitive element has no effect on the antenna performance, whereas an inductive element exhibits a behavior similar to the stub loadings. Figure 8 shows the curves of reflection coefficient versus frequency for several values of inductors connected in the place of stubs. Comparison of the Γ-f curves in Figures 5(a)

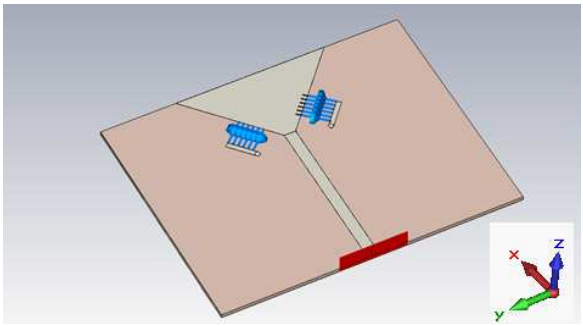

Figure 7. Replacement of combline stub loading by appropriate lumped inductors.

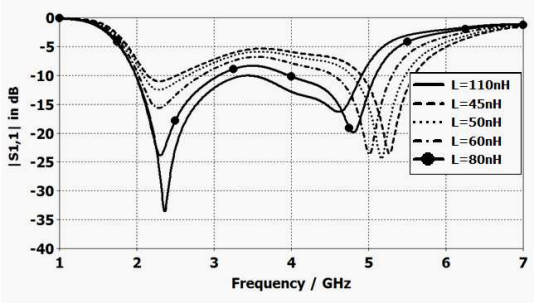

Figure 8. The reflection coefficient versus frequency of the antenna in Figure 7.

and 8 indicates the correspondence between the combline stubs and inductive loadings of PTM antenna. Observe that longer stubs provide longer paths for currents resulting in stronger inductive loadings. Consequently, combline stubs provide strong parallel inductive loadings at the patch edges.

Placement of symmetrical stubs on the patch edges leads to effective cancelation of cross-polarized radiation fields, which may be observed in Figure 6(d). The current components in the y-direction on the combline stubs on the two edges of PTM patch are in opposite directions, and consequently cancel the effects of each other, which may be the cause of radiation by cross-polarizations.

Consequently, we have a method in the form of simple combline loadings to increase the number of resonance frequencies of an antenna and vary their locations by adjusting the geometrical dimensions of stubs.

4. DESIGN OF DUAL-BAND AND WIDEBAND PTM ANTENNA

We now proceed to employ the combline stub loadings of PTM antenna to obtain dual-band and wideband performance.

First, we design it for WLAN systems to operate at two frequency bands, namely 2.4 GHz and 5 $\sim$ 6 GHz. We use the basic PTM antenna as designed in Section 3 for the first band of WLAN, namely 2.4 GHz. We then use the proposed method of inductive loading of antenna to

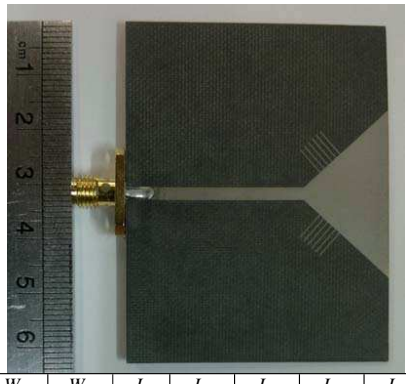

W	W_1	W_2	L	L_1	L_2	L_3	L_4	n
49	2.37	31.5	63	33.4	32.5	2.8	4	6

Figure 9. Fabricated prototype of loaded PTM antenna for WLAN application. Dimensions are in millimeters.

make it operate at the second WLAN frequency band $5 \sim 6\,\text{GHz}$. Accordingly, we refer to the results of Section 3 and the frequency responses given in Figure 5. The selected substrate is RT5880. We select the initial values of parameters as stub length $L_3 = 6\,\text{mm}$, stub offset $L_4 = 4.5\,\text{mm}$, number of stubs $n = 4$ and stub spacing $d = 1\,\text{mm}$. The optimizer using the genetic algorithm in the CST simulation software is employed to determine the optimum values of the above parameters, which are tabulated in Figure 9. A photograph of its prototype model is also shown in Figure 9. The simulation results and measurement data for its and its various radiation patterns and reflection coefficient are given in Figures 10 and 11 respectively. The method in Figure 7 shows that the inductive loading by stubs may be achieved by an inductor of 40 nH.

The minor discrepancies between the simulation and measurement data may be attributable to fabrication tolerances and simulation limitations. The reflection coefficient is less than $-10\,\text{dB}$ at the lower

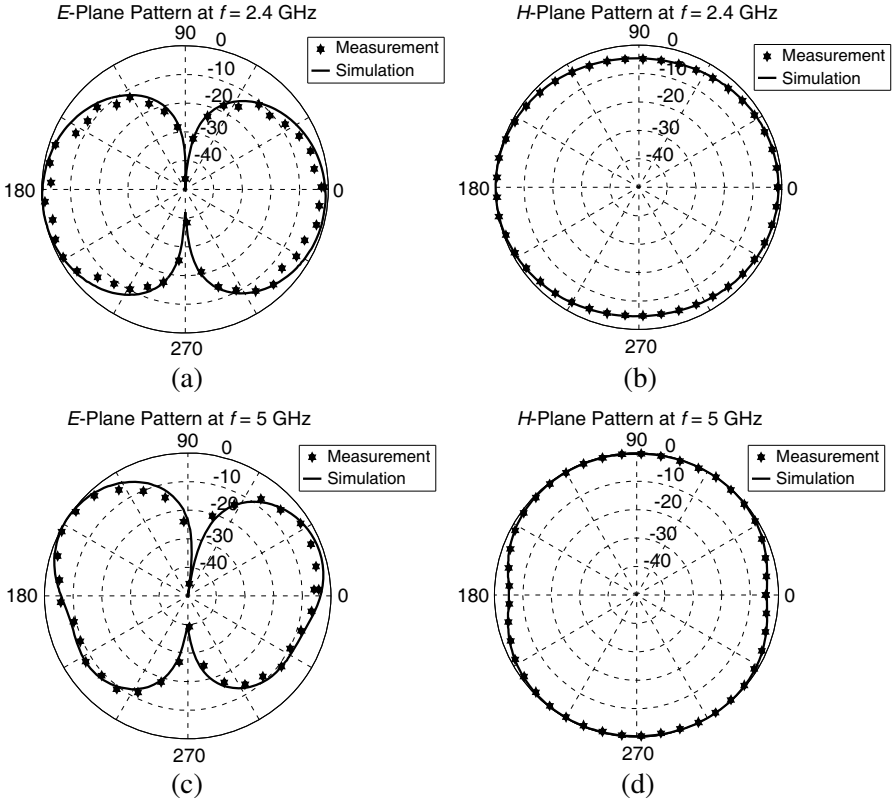

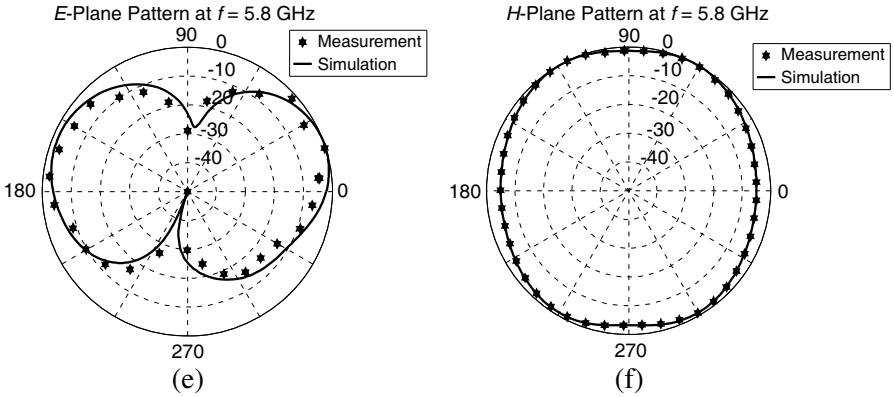

Figure 10. Normalized patterns of loaded PTM antenna for WLAN. At 2.4 GHz: (a) E-plane (xoz); (b) H-plane (yoz). At 5 GHz: (c) E-plane (xoz); (d) H-plane (yoz). At 5.8 GHz: (e) E-plane (xoz); (f) H-plane (yoz).

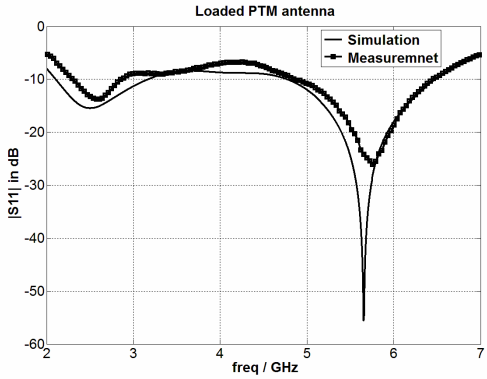

Figure 11. Simulated and measured reflection coefficient of PTM antenna for WLAN application.

and higher frequency bands 2.4 GHz and 4.9 $\sim$ 6 GHz. Consequently, this antenna is quite suitable for use in WLAN systems. The lower band is quite narrow and does not pose any problems, but the higher band is somewhat wide and for its acceptable performance, the number of stubs should be quite high, which is selected here equal to 6. The radiation patterns are given at three frequencies across the WLAN band, namely (2.4, 5, 5.8) GHz. The antenna gains at 2.4 GHz and 5.5 GHz are about 2.9 dBi and 3.1 dBi respectively.

The placement of combline stubs as inductive loadings is less effective at the lower frequency, for the cancelation of cross-polarized radiation fields. The cross-polar radiation patterns of the PTM antennas with and without stub loadings for the lower frequency are drawn in Figure 12, which show no significant difference between them.

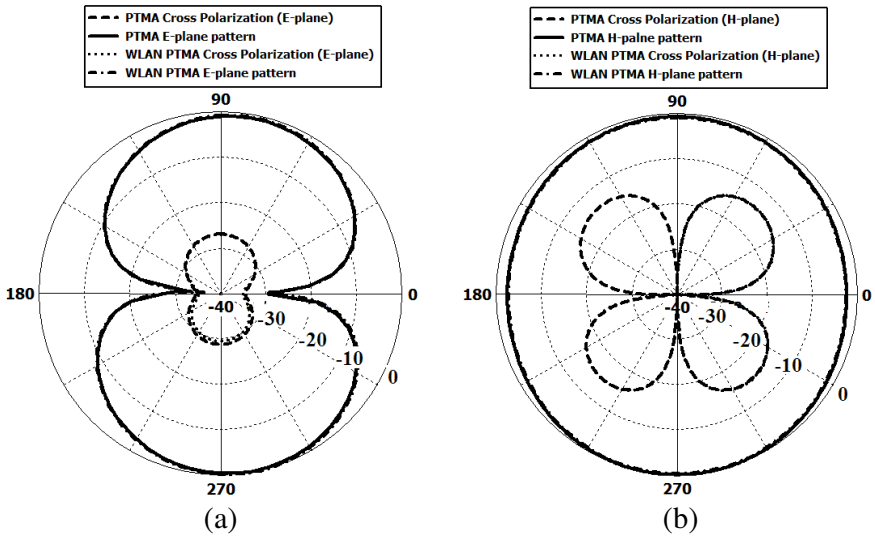

Figure 12. Comparison of simple and stub loaded PTM antenna cross polarization at 2.4 GHz. (a) E-pane; (b) H-pane.

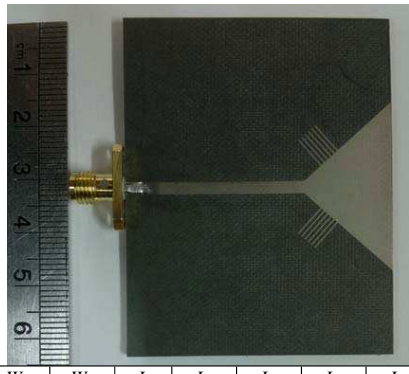

W	W_1	W_2	L	L_1	L_2	L_3	L_4	n
49	2.37	31.5	63	33.4	32.5	4	3.5	6

Figure 13. Fabricated prototype of wideband PTM antenna. Dimensions are in millimeters.

Second, we consider the design of the combline loadings of a PTM antenna for a wideband performance. Since the variation of stub lengths may change the location of second resonance frequency of antenna, then we may try to let it approach the first resonance frequency by a judicious choice of stub lengths and realize a wide frequency band performance. The increase of stub lengths may decrease the second resonant frequency, as indicated by a parameter sweep in Figure 5(a). By a proper design through computer simulation, we may arrive at an antenna which has achieved a 90% bandwidth. Its dimensions are tabulated in Figure 13.

The selected substrate is RT5880. A photograph of its fabricated prototype model is also shown in Figure 13. The simulation results and measurement data for its various radiation patterns and reflection coefficient are given in Figures 14 and 15 respectively. They are in good agreement. The antenna gains at 2.4 GHz and 5 GHz are about

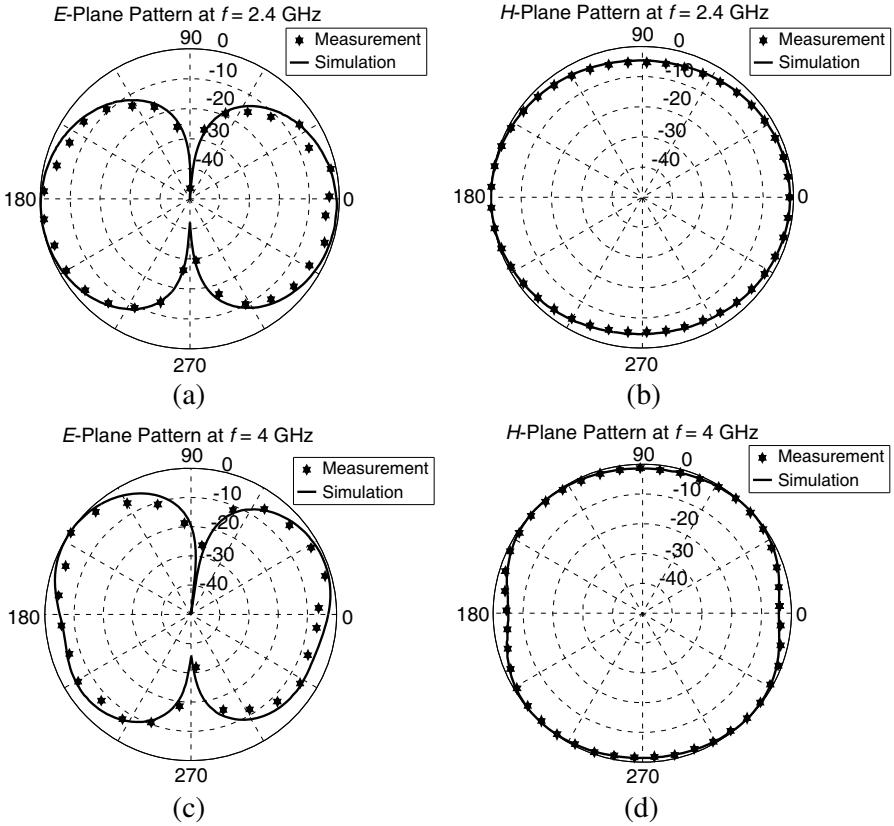

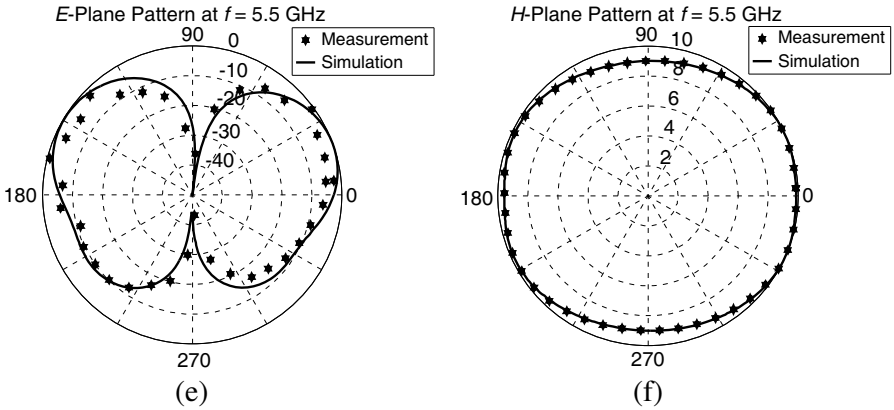

Figure 14. Normalized patterns of wideband PTM antenna for WLAN. At 2.4 GHz: (a) E-plane (xoz); (b) H-plane (yoz). At 4 GHz: (c) E-plane (xoz); (d) H-plane (yoz). At 5.5 GHz: (e) E-plane (xoz); (f) H-plane (yoz).

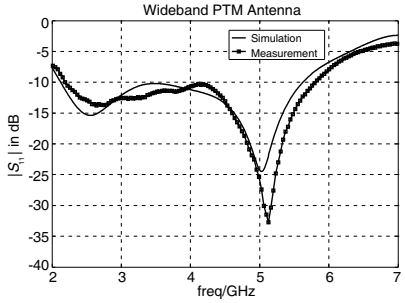

Figure 15. Simulated and measured reflection coefficient of the wideband PTM antenna.

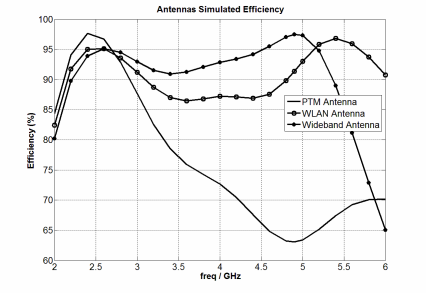

Figure 16. Simulated efficiency of the three prototype antennas.

2.85 dBi and 3.35 dBi, respectively.

The method in Figure 7 shows that the equivalent inductive loading of PTM may be achieved by 100 nH inductors. Furthermore, combline stub loading of PTM does not produce objectionable cross-polarization.

The radiation efficiencies of the aforementioned PTM, WLAN type and wideband antennas are computed by CST simulation software and are drawn in Figure 16. Observe that in the lower frequency band,

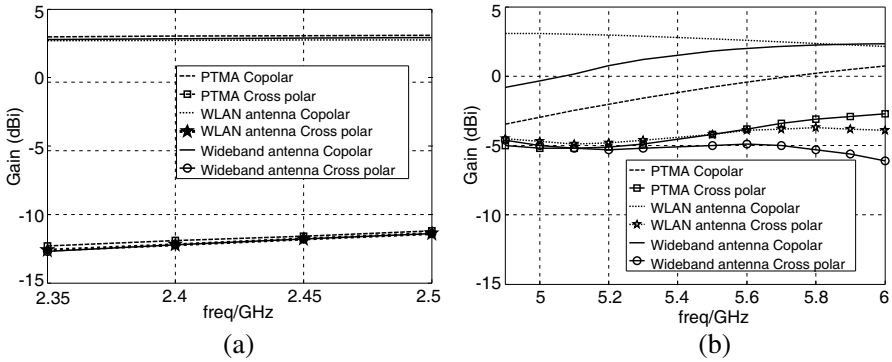

Figure 17. Gain variation versus frequency. (a) First band; (b) second band.

the efficiency of the PTM antenna is somewhat higher than those of the other two antennas. But it drastically decreases somewhat towards higher frequencies. The efficiency of WLAN antenna is about 95% in the upper band. That of the wideband antenna is higher than 90% in the frequency band $2.3 \sim 5.2$ GHz.

The gain of the three antennas (PTMA, WLAN, Wideband) for the co polar and cross polar radiation patterns in the two frequency bands are drawn in Figure 17, as obtained by computer simulation.

The gain of the co polar case is obtained for the broadside and that of the cross polar case is the maximum value (obtained at any direction of beam). Observe that in the first band, the gain of cross polar case is 10 dB less than that of co polar case. In the second band, this value is reduced to about 5 dB.

5. CONCLUSIONS

It is demonstrated that inductive loadings of a PTM antenna in the form of combline stubs may be used to realize dual-band and wideband microstrip antennas for application in WLAN. This concept of combline loadings may be applied to any planar patch shape. General configurations of combline stubs may be used, where the stub widths, lengths, spacings and locations may be assumed variable to derive the optimum performance for specified design goals. It is shown that the combline inductive loadings of patch antennas may readily realize multiband performance and are actually easily fabricated by available photolithography technology.

REFERENCES

1. Ammann, M. J., "Square planar monopole antenna," *Inst. Elect. Eng. NCAP*, No. 461, 37–40, IEE Publication, York, UK, 1999.
2. Ammann, M. J., "Control of the impedance bandwidth of wideband planar monopole antennas using a beveling technique," *Microwave Opt. Technology Letter*, Vol. 30, No. 40, 229–232, Aug. 2001.
3. Ammann, M. J. and Z. N. Chen, "Wideband monopole antennas for multi-band wireless systems," *IEEE Antennas Propagt. Mag.*, Vol. 45, No. 2, 146–150, Apr. 2003.
4. Wu, X. H. and Z. N. Chen, "Comparison of planar dipoles in UWB applications," *IEEE Trans. Antennas Propagt.*, Vol. 53, 1973–1983, Jun. 2005.
5. Agrawall, N. P., G. Kumar, and K. P. Ray, "Wide-band planar monopole antennas," *IEEE Trans. Antennas Propagt.*, Vol. 46, 294–295, Feb. 1998.
6. Brown, G. H. and O. M. Woodward, "Experimentally determined radiation characteristics of conical and triangular antennas," *RCA Rev.*, Vol. 13, No. 4, 425–452, Dec. 1952.
7. Wong, K. L. and Y. F. Lin, "Stripline-fed printed triangular monopole," *Electron. Lett.*, Vol. 33, 1428–1429, Aug. 1997.
8. Lee, J. P., S. O. Park, and S. K. Lee, "Bow-tie wideband monopole antenna with the novel impedance-bandwidth technique," *Microwave Opt. Technology Letter*, Vol. 36, No. 40, 448–452, Jun. 2002.
9. Johnson, J. M. and Y. Rahmat-Samii, "The tab monopole," *IEEE Trans. Antennas Propagt.*, Vol. 45, 187–188, Jan. 1997.
10. Lee, K. F., S. L. S. Yang, and A. A. Kishl, "Dual- and multi-band U-slot antenna," *IEEE Transactions on Antennas and Propagation Lett.*, Vol. 7, 645–647, 2008.
11. Lee, K. F., K. M. Luk, T. Mak, and S. S. L. Yang, "Dual and triple band stacked patch antennas with U-slots," *Proceedings of the 2010 EuCap Conference*, Apr. 2010.
12. Lin, C.-C. and H.-R. Chuang,"A 3–12 GHz UWB planar triangular monopole antenna with ridged ground-plane," *Progress In Electromagnetics Research*, Vol. 83, 307–321, 2008.
13. Ray, K. P., G. Kumar, and P. V. Anob, "Wide band planar modified triangular monopole antennas," *MOTL*, Vol. 49, No. 1, Mar. 2007.

14. Lin, C. C., Y. C. Kan, L. C. Kuo, and H. R. Chuang, "A planar triangular monopole antenna for UWB communication," *IEEE Microwave and Wireless Components Letters*, Vol. 15, No. 10, Oct. 2005.
15. Eldek, A. A., "Numerical analysis of a small ultra wideband microstrip-FED tap monopole antenna," *Progress In Electromagnetic Research*, Vol. 65, 59–69, 2006.
16. Liu, W.-C. and C.-F. Hsu, "CPW-FED notched monopole antenna for umts/imt-2000/WLAN applications," *Journal of Electromagnetic Wave and Applications*, Vol. 21, No. 6, 841–851, 2007.
17. Gao, S. and A. Sambell, "A simple broadband printed antenna," *Progress In Electromagnetic Research*, Vol. 60, 119–130, 2006.
18. Chen, X. and K. Huang, "Wideband properties of fractal bowtie dipoles," *Journal of Electromagnetic Wave and Applications*, Vol. 20, No. 11, 1511–1518, 2006.
19. Zhou, H. J., Q. Z. Liu, J. F. Li, and J. L. Guo, "A swallow-tailed wideband planar monopole antenna with semi-elliptical base," *Journal of Electromagnetic Wave and Applications*, Vol. 21, No. 9, 1257–1264, 2007.